Article:
Inam, A, Drummond-Brydson, R and Edmonds, DV (2015) Effect of starting microstructure upon the nucleation sites and distribution of graphite particles during a graphitising anneal of an experimental medium-carbon machining steel. Materials Characterization, 106. 86 - 92. ISSN 1044-5803

https://doi.org/10.1016/j.matchar.2015.05.014

*Title Page

Effect of Starting Microstructure upon the Nucleation Sites and Distribution of Graphite Particles during a Graphitising Anneal of an Experimental Medium-Carbon Machining Steel

A. Inam [a], R. Brydson [a] and D.V. Edmonds [a]

[a] Institute for Materials Research
School of Chemical and Process Engineering
University of Leeds
Leeds, LS2 9JT
United Kingdom

Author email addresses: aqil inam **[**aqil.ceet@pu.edu.pk]; Rik Brydson [mtlrmdb@leeds.ac.uk]; David Edmonds [d.v.edmonds@leeds.ac.uk]

Corresponding Author:

David V Edmonds FREng FIMMM CEng CSci FASM

Professor Emeritus and Visiting Research Professor

Institute for Materials Research

School of Chemical and Process Engineering

University of Leeds

Leeds LS2 9JT

United Kingdom

tel: +44 (0)113 343 2426 (Institute Secretary: Marie Gray)

fax: +44 (0)113 343 2384

email: d.v.edmonds@leeds.ac.uk

Abstract

The potential for using graphite particles as an internal lubricant during machining is considered. Graphite particles were found to form during graphitisation of experimental medium-carbon steel alloyed with Si and Al. The graphite nucleation sites were strongly influenced by the starting microstructure, whether ferrite-pearlite, bainite or martensite, as revealed by light and electron microscopy. Favourable nucleation sites in the ferrite-pearlite starting microstructure were, not unexpectedly, found to be located within pearlite colonies, no doubt due to the presence of abundant cementite as a source of carbon. In consequence, the final distribution of graphite nodules in ferrite-pearlite microstructures was less uniform than for the bainite microstructure studied. In the case of martensite, this study found a predominance of nucleation at grain boundaries, again leading to less uniform graphite dispersions.

Keywords: Free-machining steel; Graphitization; Ferrite/Pearlite; Bainite; Martensite.

Highlights

- The potential for using graphite particles as an internal lubricant during the machining of carbon steels is explored via the metallography of their formation during a high temperature anneal of an experimental steel composition.

- The influence of the pre-anneal starting microstructure on the nucleation sites of the graphite particles is demonstrated.

- The influence of the pre-anneal starting microstructure on the distribution of the graphite particles is also investigated.

- These microstructural features are expected to be influential on whether graphite particles, rather than carbide particles, would improve machinability, thus allowing beneficial new free-cutting steel compositions to be developed without enhanced or special alloying additions such as Pb.

1. Introduction

Steel is a high volume industrial material and in consequence, to enable rapid forming and also minimise costs, various steels have been developed which allow machining at higher cutting speeds [1,2]. Known as free-cutting or free-machining steels these steel grades generally contain enhanced or special alloying additions (e.g. Pb, S, P, Bi, Se, Te) which can make them difficult to process or re-cycle, and as more stringent health and safety legislation is introduced might eventually lead to their restriction or total prohibition from certain manufactured products [1-5]. Consequently, should more process- and user-friendly economic alternatives be discovered it is most likely that their adoption would quickly follow. One simple alternative, if a steel chemistry and process route compatible with high-volume mass production can be devised, is to use carbon in its equilibrium form, graphite, as an internal lubricant [e.g. 5]. The present article reports upon part of a project to develop experimental machining steels designed to graphitise during a relatively short anneal [6-17]. Thus it has been demonstrated that the kinetics of graphitisation can be markedly accelerated by deliberately alloying medium-carbon steel with the graphitising elements Si and Al. The primary objective of this part of the study is to determine the effect of starting microstructure upon the nucleation sites and distribution of graphite particles in three starting microstructures; ferrite-pearlite, bainite and martensite. At present, there is no such data available comparing the effect of starting microstructure on the graphite nucleation sites and their distribution, which may influence machinability, in carbon steels. In consequence, a detailed microstructural characterisation study was carried out using light optical and electron microscopy techniques. Comparisons between the influence of the different starting microstructural conditions on graphite dispersion and hence machinability will be reported elsewhere.

2. Material and Methods

The experimental steel studied was a medium-carbon steel containing relatively high Si and Al content and was prepared as a 60 kg heat at Tata Steel, Rotherham, UK. The analysis is given in Table 1.

The ingots produced were hot-rolled to plate of 12 mm thickness. In order to perform the various heat-treatments for microstructural study, small specimens ~10 mm^3 were cut using a Struers Discotom 2 cutter flooded with cooling fluid to prevent specimen heating. A heat-resistant Oxy-Stop 2200 coating to assist with protection against mill-scale (iron oxide) formation was also used.

Three typical starting microstructural conditions were considered:

- Ferrite/pearlite (as-received hot-rolled and normalised condition).
- Bainite (austenitised 1150 °C for 7 minutes and austempered at 400-420 °C for 60 minutes in a nitrate salt bath).
- Martensite (austenitised 1150 °C for 7 minutes and water quenched).

Samples for metallographic study were then annealed (tempered) at 680 ºC for increasing times (~20 minutes to ~720 minutes (12 hours)).

For microscopic analysis by light and scanning electron microscopy specimens were prepared by standard metallographic procedures before etching in 2% Nital. The light optical microstructural study was carried out using an Olympus BX51 microscope and digital micrographs recorded with an AxioCam MRc 5 (Carl Zeiss) camera attached to the microscope. Specimens prepared for light optical microscopy were also used for secondary electron (SE) imaging and EDX (energy dispersive X-ray spectroscopy) on a LEO 1530

Gemini FEGSEM equipped with an energy dispersive X-ray spectrometer. SE imaging and EDX were carried out at 10 kV.

3. Results and Discussion

3.1 Light Optical Microscopy

3.1.1 Ferrite-Pearlite Starting Microstructure

Micrographs of un-etched and etched microstructures showing the sequence of graphitisation from the ferrite-pearlite starting microstructure of the experimental steel are presented in Fig. 1. The typical ferrite-pearlite starting microstructure before annealing can be seen in Fig. 1(a). The coarse and irregular morphology of the individual particles or nodules formed is distinctive of graphite, as observed by separate studies of this experimental steel composition (6-17), as well as being suggestive of early nucleation at inclusion particles in the steel.

The sequence of micrographs in Fig. 1 also shows evidence for spheroidisation of lamellar pearlitic cementite within the pearlite regions and its eventual dissolution, and the formation of an equiaxed ferrite matrix from the original starting microstructure. After 8 hours this process appears to be complete with little carbide observable by light optical microscopy and only coarse graphite particles inhabiting an equiaxed ferrite matrix.

A graphite particle embedded in a pearlite colony, as shown in Fig. 1(b), is typical and indicates these as favoured nucleation sites, given the proximity to the cementite as the source of carbon, and also the lamellae boundaries as diffusion pathways. However, also evident from closer inspection is that many of the coarse graphite nodules in the ferrite-pearlite microstructure contain particles near their centre, as can be seen, for example, in Figs. 1(b), (f) and (g)). It is known that graphite can nucleate on particles, often nitrides or oxides [18-20]. These are often the first nucleation sites to operate, and lead to a coarse dispersion of more irregular graphite nodules. If other sites, such as individual tempering and coarsening carbide particles, as suggested and investigated by He et al. [6-16], are not activated this will be the final form of dispersion, which appears to be the case in the ferrite-pearlite starting microstructure. However, it is then interesting to speculate as to why, if the nucleation is promoted by such nucleating particles, so many of the nodules grow in association with the pearlite regions. This may be because a majority of nucleating particles exist in these regions, or that there is competition for carbon in the early stages of nucleation and growth, with the nodules located in pearlite regions dominating because of the dissolution of the high volume fraction of cementite as the principle source of carbon.

The micrographs in Fig. 1 also contain clear evidence for association of the graphite particles with ferrite grain boundaries, and so it is likely that these influence strongly the nodule growth and largely contribute to the irregular morphology during the later stages of growth.

3.1.2 Bainite Starting Microstructure

The bainite microstructure developed at 400 ºC in the experimental steel is shown in Fig. 2(a) and a magnified image of the cluster of ferrite plates from the outlined region reproduced in Fig. 2(b). The roughly parallel packets of ferrite plates, visible in Fig. 2(b), are also referred to as sheaves and have a length ~10 µm. These feathery ferrite crystals revealed in Fig. 2 were identified as upper-bainite microstructure according to previous metallographic studies as, for example, reviewed recently by Furuhara [21], and Caballero for steels with enhanced Si concentrations [22]. From detailed observations by high-resolution electron microscopy made by He et al. [6-16] it is assumed that tempering bainitic carbides, which would be coarsening rapidly during the graphitising anneal, can act as the nuclei for graphite particles, thus leading to the apparently more refined graphite dispersion obtained as compared with the ferrite-pearlite starting microstructure. Etched microstructures, developed after 30 minutes and 4 hours of graphitising anneal from the bainite starting microstructure, are presented in Figs. 2(c) and (d), respectively.

These reveal a similar graphite size and distribution suggestive that little further graphitisation occurs after the shorter anneal. The graphite particles are more regular in morphology and the dispersion is more refined and relatively uniform as compared with that generated from the ferrite-pearlite starting microstructure. The relatively rapid grain growth of an equiaxed ferrite matrix from the initial bainite can also be noted.

3.1.3 Martensite Starting Microstructure

Fig. 3(a) shows lath martensite developed after water quenching the experimental steel from 1150 ºC and a magnified image from the region outlined is reproduced in Fig. 3(b). This form of martensite is consistent with a report by Maki [23] that this lath martensite morphology, rather than a thin plate one, is only produced at high austenitising temperatures. The martensite laths are indicated by arrowheads in Fig. 3(b), and as far as can be determined at the resolution of the light optical microscope, appear to have widths ~0.5 μm, also consistent with detailed metallography by Maki [23]. The etched microstructures developed after 30 minutes and 1 hour of graphitising anneal are shown in Figs. 3(c) and (d), respectively. It appears very clear from this set of micrographs that the graphite particles were not uniformly distributed in the ferrite matrix but positioned at present or previous positions of grain boundaries. It is expected that this striking observation of grain boundary precipitation of graphite in the martensite starting microstructure would have an influence on grain size by pinning ferrite grain boundaries during growth. Certainly this distribution of graphite is very different to that in the most comparable alternative starting microstructure of bainite. Nonetheless, comparison of Figs. 2 and 3 does not give the impression of a refined ferrite microstructure from martensite as compared with bainite, although these micrographs have been selected to present different features. But this mode of graphite precipitation is a new observation because such distinctive formation along grain boundaries has not been reported previously. In consequence, this distribution and its effect upon ferrite grain size during the graphitization anneal is clearly a subject for more detailed research.

The size range of the graphite particles, however, is more similar to that also developing from the bainite, and it also appears that little further graphitisation occurs after the shorter annealing times. It is possible that some coalescence of graphite is beginning to occur by coarsening along the boundaries, although it was not possible to confirm this due to limited resolution of the light optical microscope. However, it should be mentioned that this strong association of graphite nucleation confined mainly to the grain boundary regions of the martensite starting microstructure was not apparent during previous investigations of this experimental steel [6-16] and so it is likely that a more uniform dispersion of graphite particles, more similar to that of the bainite starting microstructure, should also be possible.

The microstructural sequence observed above relates most directly to the later stage of martensite tempering at elevated temperature (in this specific case 680 ºC) as recently described, for example, by Krauss [24] and also by Maki [23]. However, it is assumed that all of the previous well-known stages of tempering also described would have occurred rapidly during the heating cycle or earlier than the first observation of the appearance of graphite. Thus it is expected that the graphite forms within a fully-tempered near-equiaxed matrix of ferrite. However, the experimental steel has been designed to contain relatively high concentrations of Si and Al which favour graphitisation rather than stabilisation of carbides. In consequence, recent studies [e.g. 16] discovered, using principally TEM/EELS techniques, that the coarse particles formed in martensite in this composition of steel by tempering at high temperatures are not fully crystalline cementite but can contain a more amorphous structure, rich in carbon. Thus it is thought that these tempering particles can act as a transitional phase which forms the initial nuclei for graphite, and moreover, are more numerous than the larger nitride or oxide particles which can also operate, as seen above, in the case of ferrite-pearlite structure. Consequently, these particles lead to a finer dispersion of smaller graphite particles. He et al. [e.g. 16] have also produced fairly persuasive metallographic evidence that the small spherical graphite nodules ≤5 μm diameter which are produced do not enclose a separate foreign nucleating particle within them, but instead, have a more amorphous core, more representative of the transitional partly-amorphous particles mentioned above.

3.1.4 Shape, Size and Distribution of Graphite Particles

The significant differences in graphite particle shape, size and distribution between the three starting microstructures are readily apparent from the micrographs. This is confirmed by the majority of maximum graphite particle diameters achieved in the fully graphitised state, measured approximately, as ferrite/pearlite ~10-20 µm; bainite ~5 µm; martensite ~1-2 µm.

3.2 Scanning Electron Microscopy

Scanning electron micrographs and accompanying qualitative EDX analysis of suspected graphite particles formed after 30 minutes of graphitising anneal from starting microstructures of ferrite-pearlite, bainite and martensite, are presented in Figs. 4(a), (b) and (c), respectively.

The EDX spectra provide additional experimental evidence that the particles or nodules examined in detail by light optical microscopy, as reported above, during the characterisation of microstructural evolution of the experimental steel during annealing the three different starting microstructures at 680 ºC, are graphite phase, and not carbide. This is consistent with previous studies of this experimental steel composition [6-17].

4. Conclusions

Light optical and electron microscopic study revealed that the graphite dispersions and final ferrite matrix resulting from a graphitising anneal of the experimental steel at 680 ºC were strongly influenced by the starting microstructures viz., ferrite-pearlite, bainite or martensite. Most noteworthy are:

- Graphite dispersion was identified in all three starting microstructures of the experimental steel by light optical microscopy of un-etched surfaces, by EDX analysis in SEM after only 30 minutes of annealing.

- The micrograph sequences strongly indicated that the favoured location for graphite particle nucleation in ferrite-pearlite starting microstructure was the pearlite regions and in the martensite starting microstructure was associated with the grain boundaries. In the bainite starting microstructure precipitation of larger graphite particles (~5 µm) were evident at the bainitic ferrite plate boundaries.

- For the experimental steel in the conditions examined, a more uniform distribution of the graphite particles resulted from the bainite starting microstructure, whilst the graphite nucleation behaviour revealed for the ferrite-pearlite and martensite starting microstructures resulted in non-uniform dispersions.

Acknowledgements

We are grateful to Tata Steel, Rotherham, UK, for providing the experimental steel for this investigation. Aqil Inam is also indebted to the University of the Punjab, Lahore, Pakistan for financial support whilst undertaking this research.

References

[1] Trent EM, Wright PK. Metal cutting. 4th ed. Boston: Butterworth-Heinemann; 2000.

[2] Childs THC, Maekawa K, Obikawa T, Yamane Y. Metal machining: Theory and applications. London: Arnold; 2000.

[3] Lampman SR, Zorc TB. Properties and selection: Irons, steels and high performance alloys; Metals Handbook. Materials Park, OH: ASM International; 1990.

[4] Akasawa T, Sakurai M, Nakamura M, Tanaka T, Takano K. Effects of free-cutting additives on the machinability of austenitic stainless steels. Mater Proc Technol 2003;143-144:66-71.

[5] Iwamoto T, Hoshino T, Amano K, Nakano Y. An advanced high strength graphitized steel for machining and cold forging uses. In: Van Tyne CJ, Krauss G, Matlock DK, editors. Fundamentals and applications of microalloying forging steels. Warrendale, PA: TMS/Minerals, Metals and Materials Society; 1996, p. 277-86.

[6] He K, Edmonds DV. On the formation of graphite nodules in the solid-state. In: Cross R, Witcomb M, editors. 15th international congress on electron microscopy, Durban, South Africa, 2002. Proceedings Vol. 1 Physical, materials and earth sciences. Microscopy Society of Southern Africa; 2002, p. 719-20.

[7] He K, Edmonds DV. A high-resolution electron microscope study of the growth structure of graphite nodules in steel. In: Cross R, Witcomb M, editors. 15th international congress on electron microscopy, Durban, South Africa, 2002. Proceedings Vol. 1 Physical, materials and earth sciences. Microscopy Society of Southern Africa; 2002, p. 667-8.

[8] He K, Brown A, Brydson R, Daniels HR, Edmonds DV. Plasmon ratio mapping of graphite spheroids in a carbon steel. In: Van Tendeloo G, editor. 13th European microscopy

congress, Antwerp, Belgium, 2004. Vol II Materials sciences. Liege: Belgian Society for Microscopy; 2004, p. 591-2.

[9] Green MJW, Reynolds PE, He K, Edmonds DV. Graphitisation of medium-carbon steel. In: Proceedings: Materials science and technology 2004, vol. I Precipitation in steels – Physical metallurgy and property development. Warrendale, PA:AIST/The Minerals, Metals and Materials Society; 2004, p. 207-15.

[10] Edmonds DV, He K. The graphitisation process in medium-carbon steel. In: Howe JM, Laughlin DE, Lee JK, Dahmen U, Soffa WA, editors. Proceedings: Solid-to-solid phase transformations in inorganic materials 2005 - Vol 1: Diffusional transformations. Warrendale, PA: TMS/The Minerals, Metals & Materials Society; 2005, p. 53-8.

[11]. He K, Edmonds DV. Acceleration of graphitisation in carbon steels to improve machinability. In: Proceedings: Super-high strength steels, 2005, Rome. Associazione Italiana di Metallurgia (AIM)/Centro Sviluppo Materiali (CSM): ISBN 88-85298-56-7 (CD-ROM); 2005.

[12] He K, Brown A, Brydson R, Edmonds DV. An EFTEM study of the dissolution of cementite during the graphitisation annealing of a quenched medium carbon steel. In: EMAG-NANO 2005: Imaging, analysis and fabriation on the nanoscale. Electron microscopy and analysis group conference, Leeds, 2005. J Physics: Conference Series 26. Bristol: IOP Publishing; 2006, p. 111–14.

[13]. He K, Edmonds DV. A potential graphitization route to improved machinability of carbon steels. In: International conference on new developments in long and forged products: Metallurgy and applications. Winter Park, Colorado, 2006. Warrendale, PA: AIST; 2006, p. 49-56.

[14] Edmonds DV, He K. Graphitization as a potential route to improved machinability of carbon steels. In: 61st ABM Annual Congress, Rio de Janeiro, Brazil; 2006. Sao Paulo: Associação Brasileira de Metalurgia, Materiais e Mineração (ABM); 2006, p. 2535-44.

[15]. He K, Brown A, Brydson R, Edmonds DV. Analytical Electron Microscope Study of the Dissolution of the Fe_3C Iron Carbide Phase (Cementite) During a Graphitisation Anneal of Carbon Steel. J Mater Sci 2006;41:5235-41.

[16] He K, Daniels HR, Brown A, Brydson R, Edmonds DV. An electron microscopic study of spheroidal graphite nodules formed in a medium-carbon steel by annealing. Acta Materialia 2007;55:2919-27.

[17] Inam A, Edmonds DV, Brydson R. Heterogeneous nucleation of graphite in carbon steel. In: Stokes DJ, Rainforth WM, editors. Proceedings: 15th European microscopy congress, Manchester, 2012.Oxford: Royal Microscopical Society; 2012, p. 495-6.

[18] Oikawa K, Abe T, Sumi S. Medium-carbon steel having dispersed fine graphite structure and method for the manufacture thereof. Patent 6174384, United States of America, 2001.

[19] Tanaka R, Yamane Y, Sekiyab K, Narutakib N, Shiragac T. Machinability of BN free-machining steeel in turning. Int J Machine Tools & Manufacture 2007;47:1971-7.

[20] Banerjee K, Vanugopalan T. Development of hypoeutectoid graphitic steel for wires. Mater Sci Technol 2008;24:1174 - 8.

[21] Furuhara T. Carbide-containing bainite in steels. In: Pereloma E, Edmonds DV, editors. Phase transformation in steels Volume 1: Fundamentals and diffusion-controlled transformations. Cambridge: Woodhead Publishing; 2012, p. 417-35.

[22] Caballero FG. Carbide-free bainite in steels. In: Pereloma E, Edmonds DV, editors. Phase transformation in steels Volume 1: Fundamentals and diffusion-controlled transformations. Cambridge: Woodhead Publishing; 2012, p. 436-67.

[23] Maki T. Morphology and substructure of martensite in steels. In: Pereloma E, Edmonds DV, editors. Phase transformation in steels Volume 2: Diffusionless transformations, high strength steels, modelling and advanced analytical techniques. Cambridge: Woodhead Publishing; 2012, p. 34-58.

[24] Krauss G. Tempering of martensite in carbon steels. In: Pereloma E, Edmonds DV, editors. Phase transformation in steels Volume 2: Diffusionless transformations, high strength steels, modelling and advanced analytical techniques. Cambridge: Woodhead Publishing; 2012, p. 126-50.

Table 1

Table 1 Chemical composition (wt. %) of the experimental steel studied.

Wt. % Element										
C	**Si**	**Mn**	**P**	**S**	**Cr**	**Mo**	**Ni**	**Al**	**B**	**N**
0.39	1.86	0.110	0.010	0.0019	0.005	0.015	0.005	1.38	0.0005	0.0022

High-resolution Figure(s)

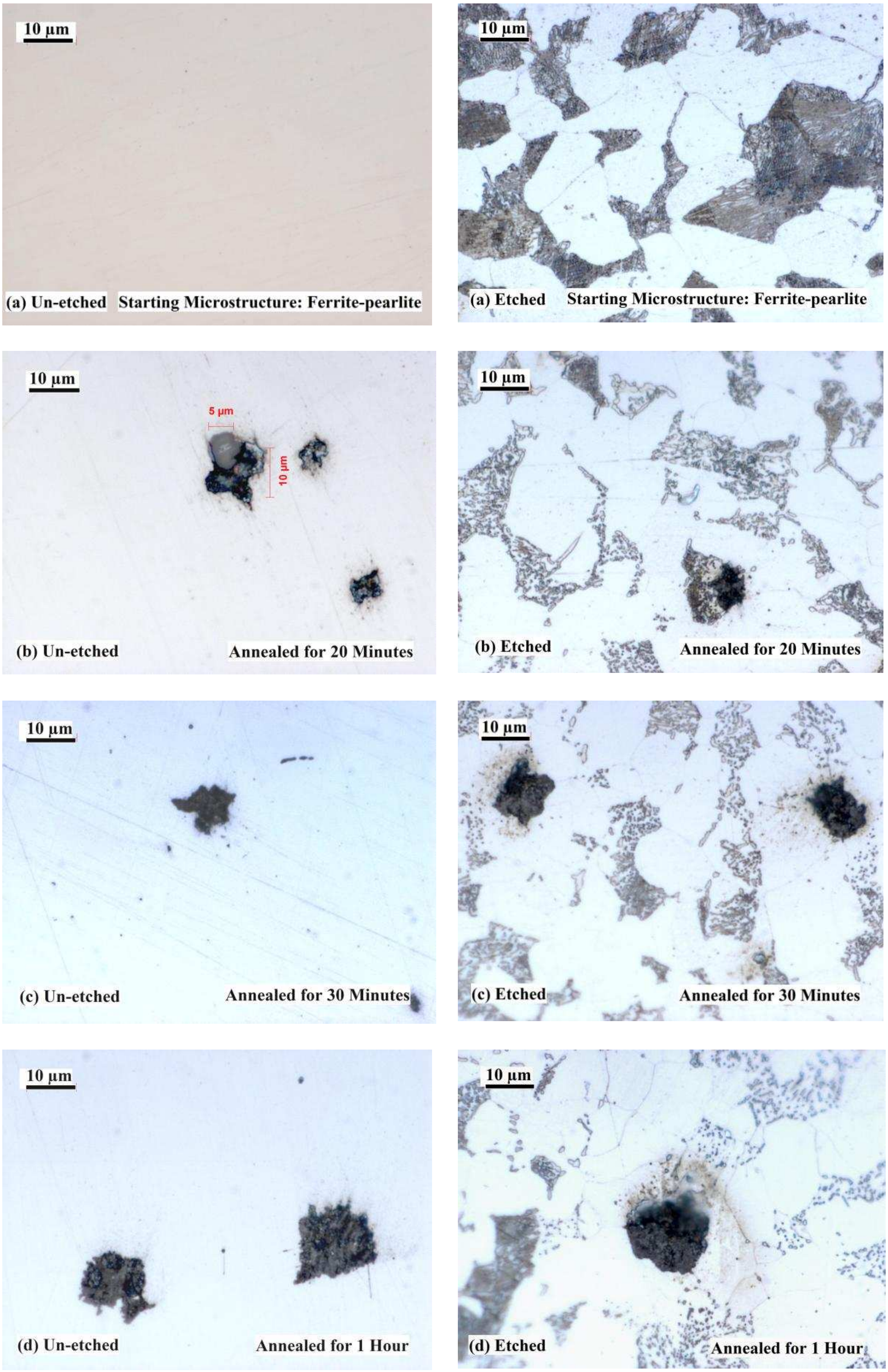

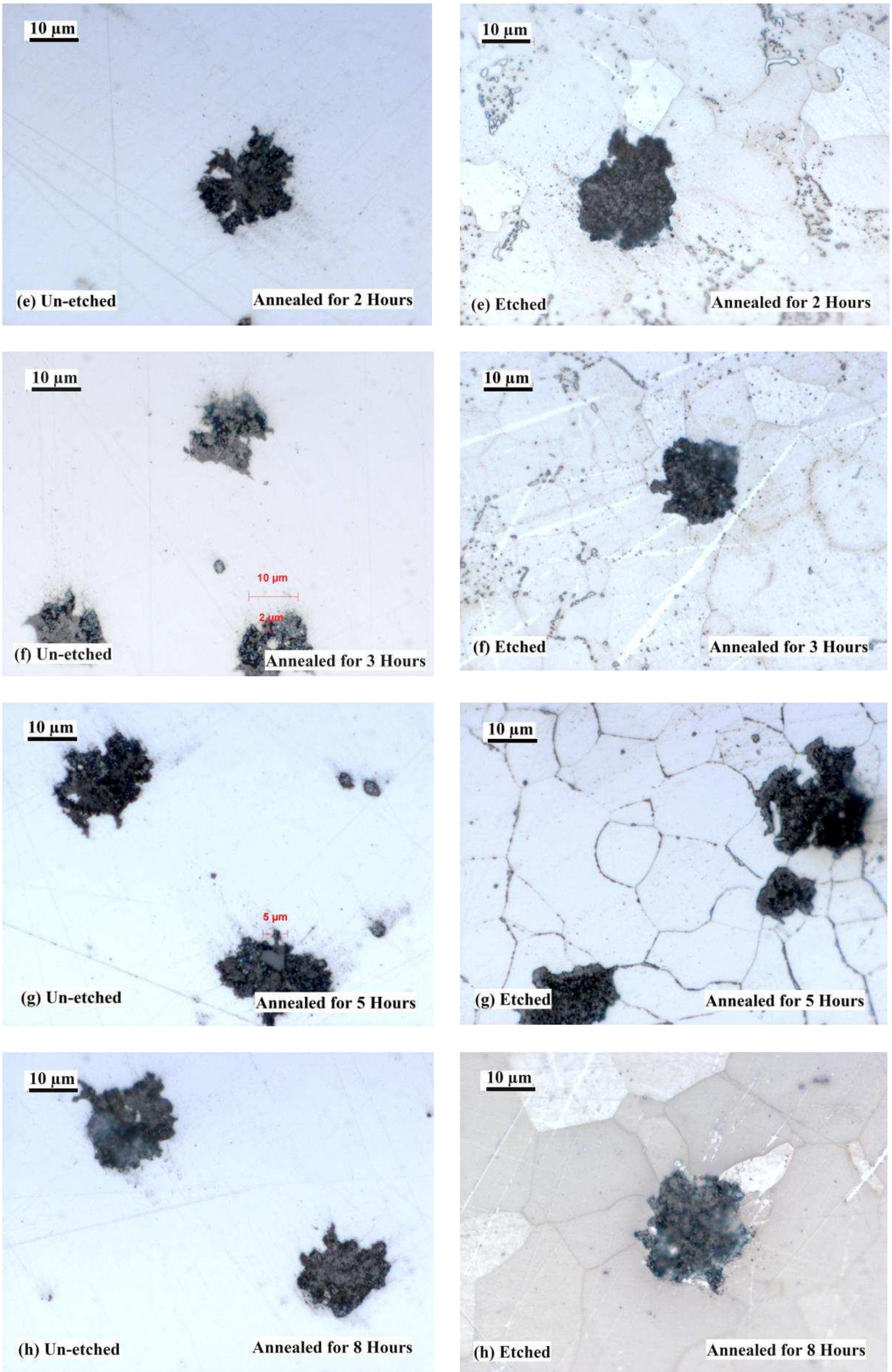
10 µm
(e) Un-etched
Annealed for 2 Hours
10 µm
(e) Etched
Annealed for 2 Hours
10 µm
10 µm
2 µm
(f) Un-etched
Annealed for 3 Hours
10 µm
(f) Etched
Annealed for 3 Hours
10 µm
5 µm
(g) Un-etched
Annealed for 5 Hours
10 µm
(g) Etched
Annealed for 5 Hours
10 µm
(h) Un-etched
Annealed for 8 Hours
10 µm
(h) Etched
Annealed for 8 Hours

High-resolution Figure(s)

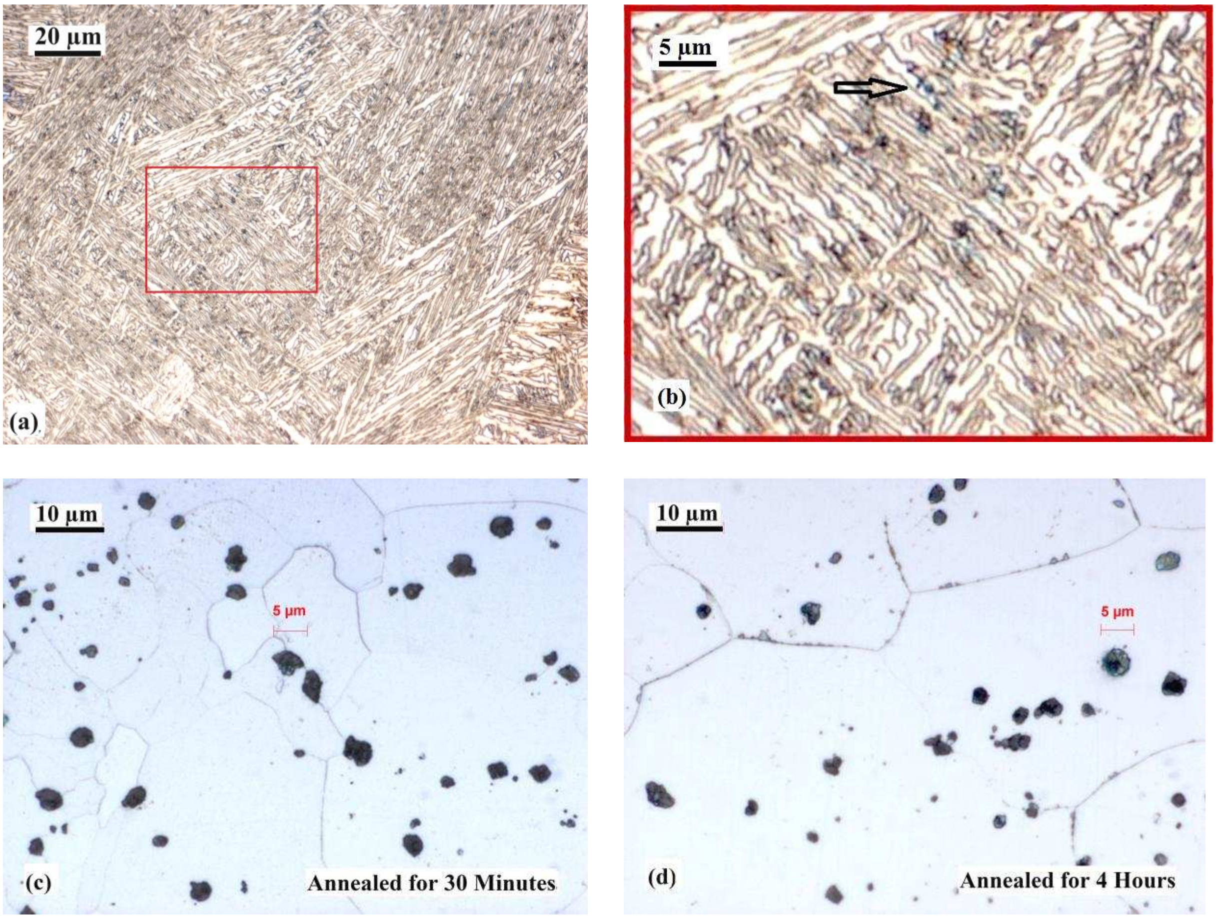

High-resolution Figure(s)

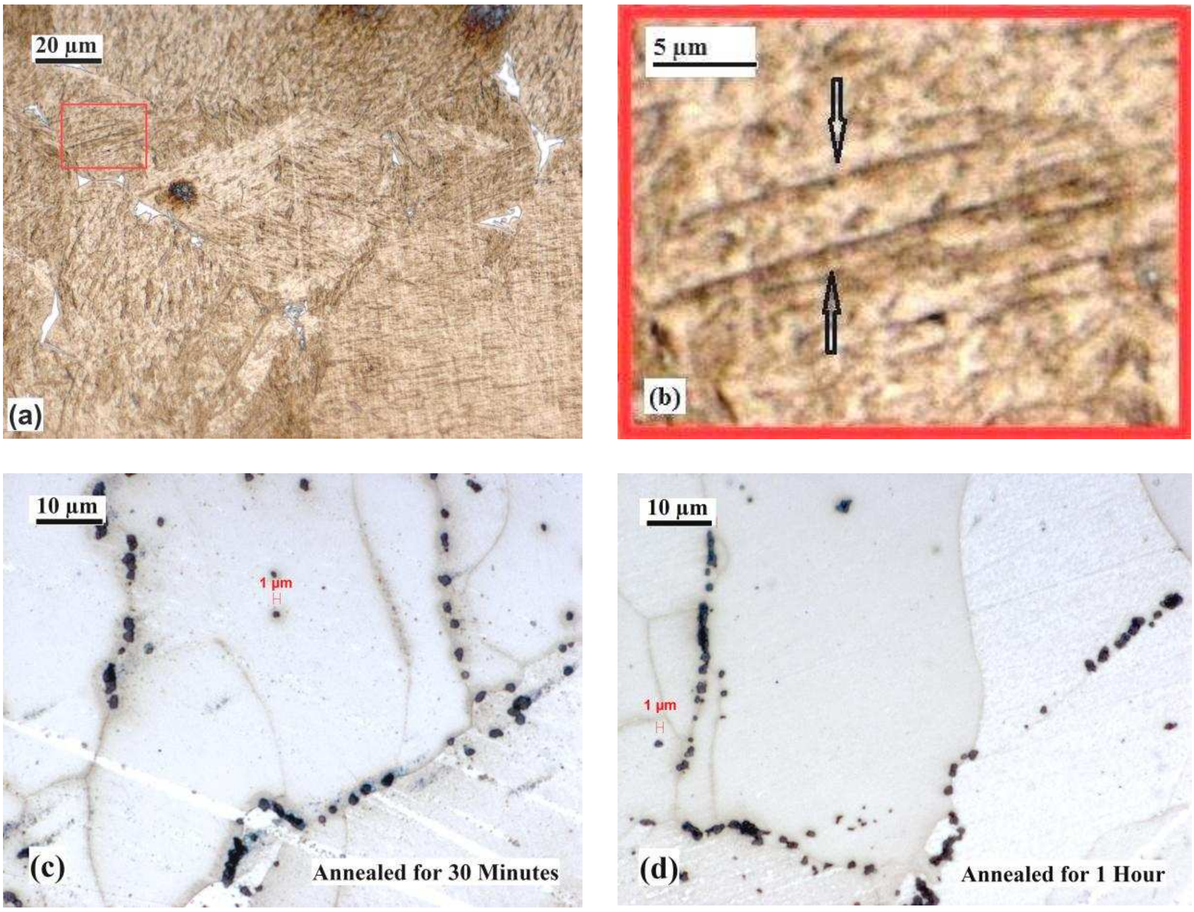

High-resolution Figure(s)